Split cylindrical gradient coil for combined PET-MR system

D. Green[1], S. Pittard[1], M. Poole[2], R. W. Bowtell[2], R. C. Hawkes[3], A. J. Lucas[3], and T. A. Carpenter[3]

[1]Varian, Inc., Yarnton, Oxfordshire, United Kingdom, [2]Sir Peter Mansfield Magnetic Resonance Centre, University of Nottingham, Nottingham, United Kingdom, [3]Wolfson Brain Imaging Centre, University of Cambridge, Cambridge, United Kingdom

Introduction

Recently there has been increased interest in developing hybrid PET-MR imaging systems, since a combination of these modalities offers co-registered functional and high resolution anatomical data, with many advantages over combined PET-CT. One such system [1,2] adopts a split magnet geometry, positioning a multi-ring PET detector array in the gap between cryostats. To further minimize the effect of the MRI system on PET detection, it is necessary for the imaging gradient coils to be split. Here we describe the design and construction of a novel 3-axis actively-shielded cylindrical gradient set for this purpose.

Design

The assembly was designed to fit an existing 1T magnet with 360mm room-temperature bore and 80mm split around the isocenter. However, the PET detector, support and light-tight assembly occupy space within the bore, so the gradient gap was required to be 110mm to accommodate these. An inner diameter of 150mm and an imaging sphere of 100mm diameter (max. gradient deviation of 5%) were chosen to match the access and field of view afforded by the PET ring. For maximum flexibility, the halves of the gradient were designed to be mechanically independent, necessitating precise alignment in the magnet bore and external electrical interconnects. Wedge clamps with unilateral access were designed to securely mount both ends of each section in the magnet bore.

Figure 1: Geometry of the split gradient coil

Methods

The magnetic design of the gradient and RT shim coils is described in [3]. It was accomplished using an Inverse Boundary Element Method (IBEM) [4], a technique that can generate coils on conducting surfaces of arbitrary geometry. In order to maximize the performance of the transverse gradient coils in the restricted space available, the annular surfaces at the split were allowed to carry current [5]. It was found that in order to achieve reasonable performance it was necessary to allow full current continuity across primary, annulus and shield surfaces. For the axial coils, the benefit derived from including the annular surfaces was not sufficient to warrant the extra construction complexity they result in.

Figure 2: Wirepaths for the x-gradient coil. Red denotes opposite sense of current flow to blue.

The axial coils were wound with heavy-gauge wire on fiberglass primary and shield formers. The transverse coils were split into primary, shield and annulus, with each section separately CNC-machined from copper sheet. Solder joints were made at the edges of the annuli for each wirepath. Copper pipe was interleaved in the structure to provide water cooling of the coils.

The two assembled halves were bolted together with spacer pillars of the correct size. The total inductance and resistance were verified, and the internal and external magnetic fields plotted using a fluxgate magnetometer mounted on an appropriate rig. Finally, the two halves were separately vacuum impregnated with epoxy resin to provide a stiff, robust structure.

Results and discussion

Table 1 summarizes the theoretical and measured performance of the gradient coils, showing good agreement for the gradient strengths and inductances, although the resistance values differ more significantly. For the X and Y coils, this is attributed to the fact that the contribution from joints between primary, annulus and shield coils is likely to have been overestimated. The fringe field and maximum deviation from linearity showed good agreement with predictions in all cases.

The gradient set will shortly be installed in the PET-MRI system in Cambridge, where its impact on PET measurements and its MR performance will be comprehensively tested.

Figure 3: Magnetic field contours generated by the x-gradient coil. The red line denotes the region of 5% homogeneity.

	Strength (mT/m/A)	Inductance (μH)	Resistance (mΩ)
X	0.66 [0.66]	111 [108]	81 [68]
Y	0.64 [0.62]	127 [121]	89 [79]
Z	0.78 [0.78]	40 [40]	43 [58]

Table 1: Gradient coil performance. Figures in brackets are measured values.

References

1. Lucas AJ, Hawkes RC, Ansorge RE, Williams GB, Nutt RE, Clark JC, Fryer TD, Carpenter TA, *Technol. Cancer Res. T.* 5:337–342 (2006).
2. Lucas A, Hawkes R, Guerra P, Ansorge R, Nutt R, Clark J, Fryer T, Carpenter A, *Proc. Intl. Soc. Mag. Reson. Med.* 15:922 (2007).
3. Poole M, *Improved Equipment and Techniques for Dynamic Shimming in High Field MRI*, Ph.D. thesis, University of Nottingham (2007).
4. Lemdiasov RA, Ludwig R, *Concept. Magn. Reson. B* 26:67–80 (2005).
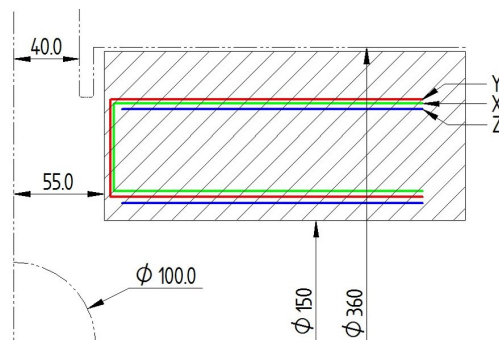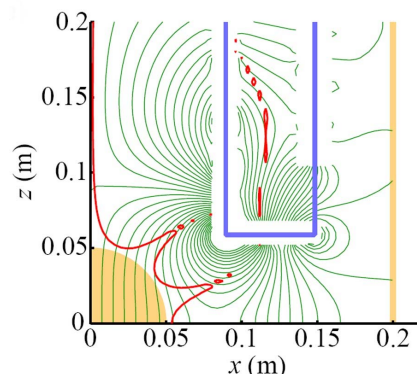5. Barber WD, Roemer PB, Rohling KW, *US Patent 5378989* (1995).